New Computational Methods for Long-Range Electromagnetic Interactions on the Nanoscale

Igor Tsukerman[*], Gary Friedman [**] and Derek Halverson [**]

[*] Department of Electrical and Computer Engineering,
The University of Akron, OH 44325-3904, USA igor@uakron.edu
[**] Drexel University, Electrical and Computer Engineering Department,
3141 Chestnut Street, Philadelphia, PA, 19104 derek.s.halverson@drexel.edu

ABSTRACT

The Flexible Local Approximation MEthod (FLAME) proposed recently by one of the authors is shown to be efficient for the simulation of long-range electromagnetic interactions between nanoparticles. Other promising applications of FLAME include charge or dipole interactions in explicit and implicit solvent models in macromolecular simulation. Mathematically, FLAME is a class of difference schemes that admit desirable accurate local approximations. A few simple tutorial-style examples are also given to elucidate the usage of FLAME.

Keywords: nanoparticle assembly; long-range forces; electrostatic interactions; magnetostatic interactions; variational-difference schemes; generalized finite-difference methods; flexible local approximation.

1 INTRODUCTION

The challenges in computing long-range electromagnetic interactions for multiple charges or particles are well known [5][12][3]. New ideas embodied in "Flexible Local Approximation MEthods" (FLAME) can lead to substantial accuracy improvements in a variety of problems.

The main advantage of FLAME is, as the name suggests, the ability to incorporate desirable accurate local approximations of the field into the global scheme. These approximations may reflect point charge or dipole singularities; boundary layers; field jumps at material interfaces, and so on. This flexibility of approximation is uncommon in traditional numerical methods. For instance, conventional Finite Difference (FD) schemes are based on Taylor expansions and do not normally take into account specific features of the solution. Finite Element (FE) methods employ piecewise-polynomial approximation and typically require complex meshes to represent the geometric and physical features of the problem.

In contrast, FLAME relies more on *algebraic* (analytical) approximation than on *geometrically* conforming meshes. The method was proposed by one of the authors and its concise description appears in [14][15]. Mathematically, FLAME is a class of variational-difference schemes. This paper describes its nanoscale applications and provides a tutorial-type illustration of its usage.

2 FLEXIBLE LOCAL APPROXIMATION

The rationale. If some features of the potential distribution – such as singularities, boundary layers, derivative jumps at material interfaces, etc. – are known *a priori*, it is desirable to introduce local basis functions representing these features. Toward this end, one needs not only a general procedure to construct difference schemes with given approximating functions, but also a convenient way of merging different approximations in different subdomains.

In the so-called Generalized FEM [2][13][10][11] approximations in different subdomains ('patches') are merged by Partition of Unity (PU). Although GFEM-PU does provide almost complete "freedom of approximation", there is a substantial price to pay for it. Multiplication by the partition of unity functions makes the approximating set more complicated, and possibly ill-conditioned or even linearly dependent [2][13]. An even greater disadvantage is the high cost of the Galerkin quadratures that need to be computed numerically in geometrically complex 3D regions [13][10].

The method. For simplicity of exposition, our focus is on the model problem in 2D or 3D

$$Lu \equiv \nabla\cdot\varepsilon\nabla u = f \qquad (1)$$

with standard types of boundary conditions in a domain Ω. Here ε is a material parameter (permittivity, permeability, conductivity, etc.) that can depend on coordinates and be discontinuous across material boundaries.

Extension of the method to the Poisson-Boltzmann equation is straightforward. What follows is a brief summary of the derivation [14], with a new focus on usage examples for FLAME. Conceptually, FLAME can be linked to multiple other methods: heuristic [19] or variational [9] homogenization; GFEM [2][13][10][11]; meshless methods [4]; and others.

The starting point is a set of overlapping 'patches' $\Omega^{(i)}$ covering the computational domain $\Omega = \cup\Omega^{(i)}$, $i = 1,2, \ldots n$. Instead of a *global* approximation space as e.g. in FEM, solution u is approximated within each patch in a separate *local* space spanned by some chosen basis functions $\psi_\alpha^{(i)}$:

$$\Psi^{(i)} = \mathrm{span}\{\psi_\alpha^{(i)}\},\ \alpha = 1,2, \ldots,\ m^{(i)} \qquad (2)$$

Multivalued approximation $u_h\{\cup\Omega^{(i)}\}$ of a given potential u is just a collection of patch-wise approximations:

$$u_h\,\{\cup\Omega^{(i)}\} \;\equiv\; \cup\{\,u_h^{(i)} \in \Psi^{(i)}\,\} \tag{3}$$

If two or more patches overlap (Fig. 1), several local approximations coexist and do not have to be the same.

Further, a regular grid with a mesh size h (for simplicity of exposition, the same in all three directions) is introduced. The i-th stencil is defined as a set of $M^{(i)}$ nodes within $\Omega^{(i)}$. Finally, the variational formulation employs a set of test functionals $\{\psi^{(i)\prime}\}$, with $\omega^{(i)} \equiv \mathrm{supp}(\psi^{(i)\prime}) \subset\subset \Omega^{(i)}$, $i = 1,2,\ldots n$.

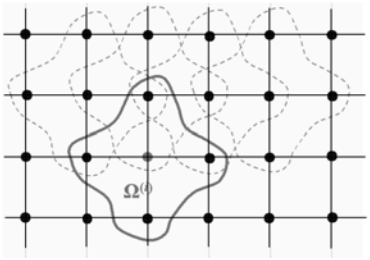

Fig. 1. Overlapping patches with 5-point stencils.

The local solution within the i-th patch

$$u_h^{(i)} \;=\; \sum\nolimits_{\alpha=1}^{m^{(i)}} c_\alpha^{(i)} \psi_\alpha^{(i)} \;\in\; \Psi^{(i)} \tag{4}$$

is required to satisfy the variational equality

$$[\,u_h^{(i)}\,,\,\psi^{(i)\prime}] \;=\; <f,\,\psi^{(i)\prime}> \tag{5}$$

where $[u, w] \equiv (Lu, w)$ and $<f, \psi^{(i)\prime}>$ is an alternative notation for $\psi^{(i)\prime}(f)$. The coefficients c are related to the nodal values of the potential via a linear transformation

$$\underline{u}^{(i)} \;= N^{(i)}\,\underline{c}^{(i)} \tag{6}$$

where $N^{(i)}$ comprises the nodal values of the basis functions on the stencil: if r_i is the position vector of node i, then

$$N^{(i)} \;=\; \begin{pmatrix} \psi_1^{(i)}(r_1) & \psi_2^{(i)}(r_1) & \ldots & \psi_m^{(i)}(r_1) \\ \psi_1^{(i)}(r_2) & \psi_2^{(i)}(r_2) & \ldots & \psi_m^{(i)}(r_2) \\ \ldots & \ldots & \ldots & \ldots \\ \psi_1^{(i)}(r_M) & \psi_2^{(i)}(r_M) & \ldots & \psi_m^{(i)}(r_M) \end{pmatrix} \tag{7}$$

If $M^{(i)} = m^{(i)}$ and $N^{(i)}$ is nonsingular, the original basis $\{\psi_\alpha^{(i)}\}$ in $\Psi^{(i)}$ can be transformed to the nodal basis $\{\,\underline{\psi}_{\mathrm{nodal}}^{(i)}\,\}$ such that $\psi_{\alpha,\,\mathrm{nodal}}^{(i)}(r_\beta) = \delta_{\alpha\beta}$:

$$\underline{\Psi}_{\mathrm{nodal}}^{(i)} \;=\; (N^{(i)})^{-T}\,\underline{\Psi}^{(i)} \tag{8}$$

where the underscores denote column vectors. The resultant difference equation of FLAME has the form [14]

$$\underline{u}^{(i)\,T}\,(N^{(i)})^{-T}\,[\underline{\Psi}^{(i)}, \psi^{(i)\prime}] \;=\; <f, \psi^{(i)\prime}> \tag{9}$$

(the functional [,] in the left hand side is applied to the column vector $\underline{\Psi}^{(i)}$ entry-wise). Graphically, the procedure can be viewed as a "machine" for generating variational-difference FLAME schemes (Fig. 2).

One implementation of this "machine" is (dropping sub- and superscripts for brevity) as follows:

1) For a given node, choose a stencil, a set of local approximating functions ψ, and a test functional ψ'.
2) Calculate the values of the ψ's at the nodes and combine these values into the N matrix (7).
3) Solve the system with matrix N^T and the r.h.s. $\underline{\Psi}$ to get the nodal basis as in (8).
4) Compute the coefficients of the difference scheme as $[\underline{\Psi}_{\mathrm{nodal}}\,,\,\psi'] \;\equiv\; (L\underline{\Psi}_{\mathrm{nodal}}\,,\,\psi')$.

Alternatively, stages 3) and 4) can be switched:

3′) Compute the values $[\underline{\Psi},\,\psi'] \;\equiv\; (L\underline{\Psi},\,\psi')$.
4′) Solve the system with matrix N^T and the r.h.s. $[\underline{\Psi},\,\psi']$ to obtain the coefficients of the difference scheme.

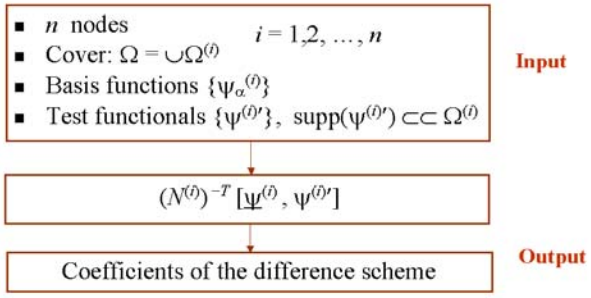

Fig. 2. A machine for variational-difference schemes.

Note that the r.h.s. of the system of equations $\underline{\Psi}$ involves *functions* $\underline{\Psi}_{\mathrm{nodal}}$ in the first version of the algorithm[1] and *numbers* $[\underline{\Psi},\,\psi']$ in the second version. While working with numbers is easier, the nodal functions can be helpful and may be reused for different test functionals.

3 TUTORIAL EXAMPLES FOR FLAME

For a tutorial-style illustration, let us consider a few examples – as simple as possible in this section and more realistic in the following one. In 1D, the setup of the overlapping patches is obvious: each $\Omega^{(i)}$ is a segment (of length between $2h$ and $4h$) containing exactly three neighboring grid nodes. Let the local basis functions over each $\Omega^{(i)}$ be $\psi_\alpha^{(i)} = \{1, x, x^2\}$. The matrix of nodal values then is

$$N^{(i)} \;=\; \begin{pmatrix} 1 & x_i - h & (x_i - h)^2 \\ 1 & x_i & x_i^2 \\ 1 & x_i + h & (x_i + h)^2 \end{pmatrix} \tag{10}$$

Next, let the test functional be $\psi^{(i)\prime} = \delta(x - x_i)$ [collocation]. Then in (9) $[\underline{\Psi}^{(i)}, \psi^{(i)\prime}] \equiv (\nabla^2\underline{\Psi}^{(i)}, \psi^{(i)\prime})$ is just the column vector $[0, 0, 2]^T$ of the second derivatives of the basis functions. The coefficients of the difference scheme are found, by solving the 3×3 system with matrix $(N^{(i)})^T$ in (9), to be the same as in the standard three-point scheme in 1D, i.e. $h^{-2}\cdot\{1, -2, 1\}$.

Quite similarly, in 2D the choice $\Psi^{(i)} = \mathrm{span}\{1, x, x^2, y, y^2\}$; $\psi^{(i)\prime} = \delta(r - r_i)$ leads, by direct calculation, to the usual scheme with a 5-point stencil. (A possible domain $\Omega^{(i)}$ containing the stencil is shown in Fig. 1.)

Next, consider the same set of five local basis functions in 2D but with a "window" test function $\psi^{(i)\prime} = \Pi(\omega^{(i)})$, where Π denotes the characteristic function of a domain (equal to one inside the domain and zero outside), and $\omega^{(i)}$

[1] Our own implementation is in symbolic Matlab™.

$\subset\subset \Omega^{(i)}$. The most natural choice of $\omega^{(i)}$ is the $h\times h$ square centered at node i. Then in (9) one has

$$[\Psi^{(i)}, \psi^{(i)\prime}] \equiv (\nabla^2\Psi^{(i)}, \psi^{(i)\prime}) = \int_{\Gamma^{(i)}} \frac{\partial}{\partial n}\Psi^{(i)} \cdot d\Gamma^{(i)}$$

where Γ is the boundary of $\omega^{(i)}$ and n is the outward normal to Γ. The boundary integrals are very easy to compute for all ψ's. Then, solving the system with $N^{(i)T}$ as prescribed by (9), one again arrives at the standard 5-point scheme.

Consider now another 2D example with a slightly more complex, 9-point, stencil. Let the local approximation space $\Psi^{(i)} = \text{span}\{1, x, x^2, y, y^2, xy, x^2y, xy^2, x^2y^2\}$. $N^{(i)}$ is a 9×9 matrix and the computational procedure obviously becomes quite tedious but is easily implemented in symbolic algebra. With collocation $\psi^{(i)\prime} = \delta(r - r_i)$, the 9-point stencil turns out to be redundant, as the standard 5-point scheme is again obtained. However, the flux balance scheme with the "window" function $\psi^{(i)\prime} = \Pi(\omega^{(i)})$ yields the 4th order scheme as shown.

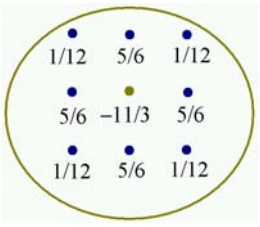

4 FLAME SCHEMES FOR PARTICLES

Given a system of local approximating functions and test functionals, the FLAME scheme is generated automatically as we have seen. The critical question then is the choice of approximating functions in each particular application.

An important case is approximation of the field at an interface between two materials with parameters ε_1 and ε_2. The normal derivative of the exact potential u has a jump

$$\varepsilon_1 \partial_n u_1 = \varepsilon_2 \partial_n u_2 \qquad (11)$$

The field is rendered continuous by the coordinate mapping

$$\tau^{\sim} = \tau, \quad n^{\sim} = n / \varepsilon \qquad (12)$$

and one can therefore expect higher approximation accuracy in the tilde-coordinates (τ is tangential to the interface). A more general mapping is rigorously analyzed in [1] (see also [9]) in 2D.

In case of a spherical particle of radius r_0, with material parameter ε_1 inside and ε_2 outside, the appropriate coordinate mapping is

$$x^{\sim} = x\, r^{\sim}/r, \quad y^{\sim} = y\, r^{\sim}/r, \quad z^{\sim} = z\, r^{\sim}/r \qquad (13)$$

where $r^{\sim} = r,\ r \le r_0; \quad r^{\sim} = r_0 + \varepsilon_1/\varepsilon_2\,(r - r_0),\ r > r_0.$

Under this mapping, the field is rendered continuous and one can therefore expect higher approximation accuracy in the tilde-coordinates. In addition, advantage can be taken of the known dipole-like behavior of the potential. Thus let

$$\Psi^{(i)} = \text{span}\ \{1, x^{\sim}, y^{\sim}, u_{\text{dipole,x}}, u_{\text{dipole,y}}\} \qquad (14)$$

where $u_{\text{dipole,x}}$, $u_{\text{dipole,y}}$ are the potentials of the particle polarized in the x- and y-direction, respectively. Away from the particles, conventional schemes for the Laplace equation can be applied.

For comparison purposes, we also use the standard flux balance scheme for hexahedral 'control volumes': the faces of the hexahedra cross grid edges at their midpoints, and the values of ε for flux balancing are evaluated at the same midpoints.

The test problem with just one particle in a uniform external field is considered first. Its well-known analytical solution was imposed on the domain boundary as the Dirichlet condition. In this case the potential inside the domain is known exactly and can be used to compute the numerical errors.

Table I shows that FLAME has much higher accuracy than the standard control volume scheme. Remarkably, even for a very crude 4×4 grid, in no way capable of resolving the particle boundary, the computed values of nodal potentials are quite accurate. This is due to the special approximating functions employed.

Similar results are obtained for a test problem with five particles (3). Since no analytical solution is easily available, an accurate FE model is used to validate the new and standard schemes (see caption of Fig. 3 for details). Again, the numerical error for FLAME is substantially smaller than for the standard control volume scheme.

TABLE I. Relative errors in the potential (Euclidean nodal norm) vs. meshsize. Cylindrical particle; $r_0 = 0.14$, $\varepsilon = 10$

Mesh	Standard scheme	FLAME with basis (14)
4	5.87E-02	4.32E-03
10×10	6.07E-03	1.39E-03
20×20	6.76E-03	2.92E-04
40×40	3.70E-03	7.57E-05
60×60	8.74E-04	3.44E-05
80×80	3.59E-04	2.02E-05
100×100	4.30E-04	1.28E-05

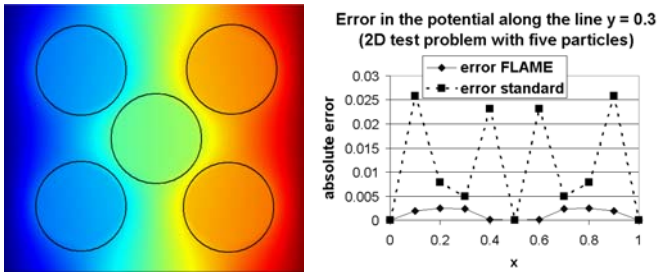

Fig. 3. Five 2D particles ($r_0 = 0.14$, $\varepsilon = 10$, coordinates of particle centers are all multiples of 0.25, unit square, Dirichlet condition $u = x$). Right: absolute errors at grid points along the line $y = 0.3$ for FLAME with spatial mapping and dipole basis and for the standard 5-point scheme. Mesh 10×10. FEMLAB solution (20736 2nd-order triangles) taken as exact.

5 DIFFERENCE SCHEMES WITH POTENTIAL SPLITTING

The ideas of FLAME are also applicable to a variety of problems in molecular dynamics, macromolecular simulation, multiparticle assembly, etc., where long-range electromagnetic interactions between charges or particles of negligible size need to be computed. For problems with 3D-periodicity [5][12], Ewald methods have been highly suc-

cessful. Still, generalized FD schemes may have advantages: ease of implementation for different boundary conditions; efficiency for massively parallel computer systems (in contrast with FFT used in Ewald methods).

Most importantly, Ewald methods cannot be applied directly to problems with inhomogeneous or nonlinear material characteristics (particles in solvent, the Poisson-Boltzmann equation, etc.). At the same time, the idea of flexible local approximation remains fully valid.

In the vicinity of each node, accurate approximation of the field can be obtained by potential splitting: the 'rough' part of the potential due to nearby sources is represented analytically and exactly, so that the FD scheme is, in effect, applied to the remaining 'smooth' part. The singular character of the rough potential has no bearing on the accuracy of the method. The computational cost is proportional to the number of particles; only real arithmetic is used; any boundary conditions (not necessarily periodic) can be easily implemented; parallelizable multilevel preconditioners rather than FFTs are employed.

Implementation details and evidence of accuracy improvement are given in [17][16] and cannot be presented here due to space limitations. Instead, we now turn to a new application of FLAME: unbounded problems.

6 TREFFTZ METHODS AND UNBOUNDED PROBLEMS

An interesting special case is a combination of FLAME with Trefftz methods where, by definition, the approximating functions satisfy the underlying differential equation exactly. Various applications of Trefftz methods have been reported in the literature; in particular, approximation of the far field as a superposition of Coulombic potentials was proposed in [7] in the FE context. We are not aware of similar methods for FD.

FLAME furnishes a matching between Trefftz-type expansions and FD schemes. If the local approximating functions satisfy the homogeneous equation $Lu = 0$ exactly, then equation (9) is automatically satisfied and becomes redundant. In its stead, one can re-interpret (6) as a constraint for the nodal values of the potential on the stencil.

More precisely, let now $M = m+1$ (dropping the node-related superscripts for brevity), where as before M is the number of nodes in the stencil and m is the number of expansion coefficients c in (4, 6); thus the matrix of nodal values N (7) has one "extra" row. Then (6) gives

$$\underline{u} \in \text{Range}\,(N) \quad \text{or equivalently} \quad \underline{u} \perp \text{Null}(N^T) \qquad (15)$$

This condition, assuming that rank(N) = m, can be used to express one of the nodal values in the stencil in terms of the others, thereby replacing the now redundant equation (9).

The accuracy, and even stability and convergence, of such a scheme of course depend on the choice of the stencil and of the approximating Trefftz set. For unbounded electro- or magnetostatic problems, Trefftz functions can be chosen as multipole potentials. Each n-pole potential function requires $(2n-1)$ stencil nodes. A practical example of the stencil [8] is shown and explained in Fig. 4. This method yields very accurate values of the potential and the field for the unbounded problem [8]. Notably, the system matrix remains sparse.

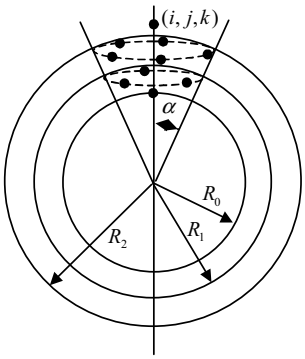

Fig. 4. An example of a stencil for a point (i,j,k) on the boundary of the exterior region. The stencil points are arranged in layers. Each stencil layer n is formed by the vertices of a $(2n-1)$-sided equilateral polygon at the intersection of the sphere of radius R_n and the cone of angle α. For n=1, the stencil point is at the axis of the cone.

7 CONCLUSION

The proposed Flexible Local Approximation MEthod (FLAME) serves as our "golden key" to substantial accuracy improvement in a large variety of nanoscale applications: particle assembly, explicit and implicit solvent models in macromolecular simulation, unbounded problems.

REFERENCES

[1] I. Babuška *et al*, *SIAM J. Numer. Analysis*, 31 (4), pp. 945-981, 1994.
[2] I. Babuška, J.M. Melenk, The partition of unity method, *Intl. J. for Numer. Methods in Engineering*, vol. 40, No. 4, pp.727-758, 1997.
[3] N.A. Baker *et al*. *PNAS* 98, No. 18, pp. 10037–10041, 2001 www.pnas.org/cgi/doi/10.1073/pnas.181342398.
[4] T. Belytschko *et al. Computer Methods in Applied Mechanics and Engineering*, vol. 139, No. 1-4, pp. 3-47, 1996.
[5] M. Deserno, C. Holm, *J. Chem. Phys.* 109 (18), pp.7678-7701, 1998.
[6] U. Essmann *et al*., A smooth particle mesh Ewald method, *J. Chem. Phys*., 103 (19), pp. 8577-8593, 1995.
[7] M.Gyimesi *et al. IEEE Trans. Magn*. 32, pp. 671-674, 1996.
[8] Derek Halverson, Gary Friedman, Igor Tsukerman, *Proceedings of the 9th Joint MMM-Intermag Conference*, Anaheim, CA, January 2004.
[9] S. Moskow *et al SIAM J. Numer. Analysis*, 36(2), pp. 442-464, 1999.
[10] A. Plaks, *et al*, *IEEE Trans. Magn*. 39, No. 3, pp. 1436–1439, 2003.
[11] L. Proekt, I. Tsukerman, *IEEE Trans. Magn*., vol. 38, No. 2, pp.741-744, 2002, and references therein.
[12] C. Sagui, T.A. Darden, *Annu Rev. Bioph. Biom.* 28, p.155-179, 1999.
[13] T. Strouboulis, I. Babuška, K.L. Copps, *Computer Methods in Applied Mechanics and Engineering*, 181, No. 1-3, pp. 43-69, 2000.
[14] Igor Tsukerman, Flexible local approximation method for electro- and magnetostatics, to appear in *IEEE Trans. Magn*., May 2004.
[15] Igor Tsukerman, Generalized finite element difference methods for electro- and magnetostatics, to appear in "*Mathematics in Industry*", Springer series, 2004.
[16] Igor Tsukerman, *Bioinformatics'2003*, Stanford, August 2003.
[17] I. Tsukerman, Efficient computation of long-range electromagnetic interactions without FT, to appear in *IEEE Trans. Magn*., 2004.
[18] B. Yellen *et al*., *J. Appl. Phys*. 91 (10), pp. 8552-8554, 2002.
[19] W. Yu and R. Mittra, *IEEE Microwave Wireless Comp. Lett*., vol. 11, pp. 25–27, Jan. 2001
[20] Z. Zhou *et al*., *J. Comp. Chem*., 11, pp.1344-1351, 1996.